References and Notes

1. R. G. Van Driesche, T. S. Bellows Jr., *Biological Control* (Chapman & Hall, New York, 1996), chap. 1.
2. H. A. Gleason, *Bull. Torrey Bot. Club* **53**, 7 (1926).
3. R. M. Callaway, *Oecologia* **112**, 143 (1997).
4. R. Turkington, L. A. Mehrhoff, in *Perspectives on Plant Competition*, J. B. Grace, D. Tilman, Eds. (Academic Press, New York, 1990), chap. 15.
5. R. Turkington, *J. Ecol.* **77**, 717 (1989).
6. L. W. Aarssen, R. Turkington, P. B. Cavers, *Can. J. Bot.* **57**, 2695 (1979).
7. L. Menchaca, J. Connolly, *J. Ecol.* **78**, 223 (1990).
8. Each of these seven species was planted alone and in all pairwise grass-*Centaurea* combinations in pots 20 cm tall and 6 cm in diameter (300 cm^2 volume) with 20 replicates per individual or species combination. The pots were filled with a 50:50 mixture 20 grit (mean diameter 0.85 mm), and 30 grit (mean diameter 0.60 mm) pure silica sand thoroughly mixed with 20 ml of soil from local Montana grasslands (to introduce microbes) in which all North American bunchgrasses and *C. maculosa* (a closely related species to *C. diffusa*) were present. Finely ground activated carbon (20 ml, without phosphorus) per 1 liter of sand was added to half of the pots with solitary grasses and with grass-*Centaurea* combinations. By mixing activated carbon into the sand in half of the pots, we established an experimental environment in which the effects of organic root exudates were reduced. Activated carbon has a high affinity for organic compounds, such as potentially toxic or "allelopathic" chemicals, and a weak affinity for inorganic electrolytes such as are found in nutrient solution (*26*), and it has previously been shown to reduce the negative effects of root exudates from other species (*15–17*). Other *Centaurea* species have been suspected to be allelopathic, and *C. maculosa*, which is very similar to *C. diffusa*, has been shown to have allelopathic root exudates [W. L. Ridenour, thesis, University of Montana, Missoula, MT, USA]. A separate experiment was conducted to examine the direct effects of activated carbon on the grasses. All plants were grown in a naturally lit growth room and supplemented with 12 hours of artificial light at ~500 $\mu mol\ m^{-2}\ s^{-1}$. Pots were watered approximately every 3 days with distilled water or a dilute nutrient solution. All plants were started from seed, and 3 months after planting seeds, the roots and shoots of all plants were harvested, dried at 60°C, and weighed.
9. We conducted a second experiment designed to test the direct effects of activated carbon on the total biomass produced by the six grass species used in the competition experiment. Each grass species was planted alone in sand with activated carbon and in sand without activated carbon (n = 7 to 9). Protocol was as in the competition experiment (*26*).
10. Analysis of variance was conducted in which the effects of region, grass genus, and carbon treatment were tested. The dependent variable was the biomass of individual grasses grown with *C. diffusa* as a percentage of the mean biomass for each species when grown alone. Region, $F(1,120) = 23.7$, $P < 0.001$; grass genus, $F(2,120) = 18.22$, $P < 0.001$; carbon, $F(1,120) = 8.35$, $P = 0.005$; region × grass genus, $F(2,120) = 0.21$, $P = 0.813$; region × carbon, $F(1,120) = 39.93$, $P < 0.001$; grass genus × carbon, $F(2,120) = 2.06$, $P = 0.132$.
11. Analysis of variance was conducted in which the effects of region (grass origin), grass genus, and carbon treatment were tested. The dependent variable was the biomass of individual *C. diffusa* grown with grasses as a percentage of the mean biomass of *C. diffusa* when grown alone. Region, $F(1,120) = 0.13$, $P = 0.719$; grass genus, $F(2,120) = 6.45$, $P = 0.002$; carbon, $F(1,120) = 2.30$, $P = 0.133$; region × grass genus, $F(2,120) = 0.17$, $P = 0.841$; region × carbon, $F(1,120) = 24.05$, $P < 0.001$; grass genus × carbon, $F(2,120) = 2.57$, $P = 0.082$.
12. To examine the effects of species and the effects of activated carbon on resource competition, we added radioactive ^{32}P to the soil in all treatments 12 days before harvesting the plants. HCl (5 ml, 0.02 M) containing 0.1 μCi of ^{32}P-labeled $KH_2{}^{32}PO_4$ as the radiation source [after M. M. Caldwell *et al.*, *Science* **229**, 384 (1985)] was injected by using a hypodermic needle into each pot 10 cm below the surface and either halfway between a single plant and the pot edge or halfway between neighbors.
13. Analysis of variance was conducted in which the effects of region, grass genus, and carbon treatment were tested. The dependent variable was the total count for ^{32}P in individual grasses grown with *C. diffusa* as a percentage of the mean count for each species when grown alone. Region, $F(1,106) = 8.46$, $P = 0.005$; grass genus, $F(2,106) = 0.71$, $P = 0.50$; carbon, $F(1,106) = 59.44$, $P < 0.001$; region × grass genus, $F(2,106) = 2.87$, $P = 0.062$; region × carbon, $F(1,106) = 69.16$, $P < 0.001$; grass genus × carbon, $F(2,106) = 1.45$, $P = 0.239$.
14. Analysis of variance was conducted in which the effects of region (grass origin), grass genus, and carbon treatment were tested. The dependent variable was the total count for ^{32}P of individual *C. diffusa* grown with grasses as a percentage of the mean biomass of *C. diffusa* when grown alone. Region, $F(1,98) = 0.01$, $P = 0.939$; grass genus, $F(2,98) = 0.18$, $P = 0.834$; carbon, $F(1,98) = 1.75$, $P = 0.190$; region × grass genus, $F(2,98) = 0.81$, $P = 0.449$; region × carbon, $F(1,98) = 18.18$, $P < 0.001$; grass genus × carbon, $F(2,98) = 1.90$, $P = 0.156$.
15. B. E. Mahall, R. M. Callaway, *Proc. Natl. Acad. Sci. U.S.A.* **88**, 874 (1991).
16. B. E. Mahall, R. M. Callaway, *Ecology* **73**, 2145 (1992).
17. O. Schreiner, H. S. Reed, *Bot. Gaz.* (February), 73 (1908).
18. Analysis of variance testing for the effects of region (origin of grasses), grass genus, and carbon treatment on total biomass produced in pots with grasses and *C. diffusa* together. Region, $F(1,120) = 4.71$, $P = 0.032$; grass genus, $F(1,120) = 0.51$, $P = 0.611$; carbon, $F(1,120) = 0.29$, $P = 0.589$; no interactions were significant (all $P > 0.30$).
19. D. A. Steenhagen, R. I. Zimdahl, *Weed Sci.* **27**, 1 (1979).
20. N. H. Fischer, L. Quijano, in *The Chemistry of Allelopathy: Biochemical Interactions Among Plants*, A. C. Thompson, Ed. (American Chemical Society, Washington, DC, 1985).
21. C. Tang *et al.*, in *Allelopathy: Organisms, Processes, and Applications*, Inderjit, K. M. M. Dakshini, F. A. Einhellig, Eds. (American Chemical Society, Washington, DC, 1995).
22. D. E. Goldberg, P. A. Werner, *Am. J. Bot.* **70**, 1098 (1983).
23. F. S. Chapin III, *Ecology* **66**, 564 (1985).
24. D. S. Wilson, *Ecology* **78**, 2018 (1997).
25. C. J. Goodnight, *Evolution* **44**, 1625 (1990).
26. P. N. Cheremisinoff, F. Ellerbusch, *Carbon Adsorption Handbook* (Ann Arbor Science Publishers, Ann Arbor, MI, 1978).

27. We thank D. Kikodze and Z. Kikvidze for their hospitality in the Republic of Georgia, help in finding elusive *C. diffusa* in Georgia, and the collection of seeds. We thank W. Hill for assistance with the isotope analysis. We gratefully acknowledge support from the National Science Foundation, DEB-9726829, and from the Andrew W. Mellon Foundation.

31 July 2000; accepted 21 August 2000

Two–Amino Acid Molecular Switch in an Epithelial Morphogen That Regulates Binding to Two Distinct Receptors

Minhong Yan,[1]* Li-Chong Wang,[1]* Sarah G. Hymowitz,[2] Sarah Schilbach,[3] James Lee,[3] Audrey Goddard,[3] Abraham M. de Vos,[2] Wei-Qiang Gao,[1] Vishva M. Dixit[1]†

Ectodysplasin, a member of the tumor necrosis factor family, is encoded by the anhidrotic ectodermal dysplasia (EDA) gene. Mutations in EDA give rise to a clinical syndrome characterized by loss of hair, sweat glands, and teeth. EDA-A1 and EDA-A2 are two isoforms of ectodysplasin that differ only by an insertion of two amino acids. This insertion functions to determine receptor binding specificity, such that EDA-A1 binds only the receptor EDAR, whereas EDA-A2 binds only the related, but distinct, X-linked ectodysplasin-A2 receptor (XEDAR). In situ binding and organ culture studies indicate that EDA-A1 and EDA-A2 are differentially expressed and play a role in epidermal morphogenesis.

Members of the tumor necrosis factor receptor (TNFR) superfamily are involved in a number of physiological and pathological responses by activating a wide variety of intracellular signaling pathways. In a database search based on sequence similarity (*1*), XEDAR was initially identified as a member of the TNFR superfamily.

[1]Department of Molecular Oncology, [2]Department of Protein Engineering, [3]Department of Molecular Biology, Genentech, 1 DNA Way, South San Francisco, CA 94080, USA.

*These authors contributed equally to this work.
†To whom correspondence should be addressed. E-mail: dixit@gene.com

The deduced amino acid sequence of XEDAR contains three cysteine-rich repeats and a single transmembrane region (Fig. 1A). XEDAR lacks an NH_2-terminal signal peptide. The presence of an in-frame upstream stop codon in both human and mouse cDNA clones indicated that the sequence shown in Fig. 1A represents the full-length open reading frame (ORF) (*1*). To confirm that XEDAR was indeed a membrane protein, we transfected MCF7 cells with either an NH_2- or COOH-terminal Flag-tagged version of XEDAR (Fig. 1B). In permeabilized cells, the expression of both tagged proteins was readily detected by anti-Flag immunostaining. However, in the absence of permeabilization, cell surface staining

was only observed in cells transfected with NH_2-terminal–tagged XEDAR, consistent with it being a type III transmembrane protein with an extracelluar NH_2-terminus and a cytoplasmic COOH-terminus (*2*). The XEDAR gene was localized to the X chromosome (*3*).

XEDAR failed to bind many known ligands of the tumor necrosis factor (TNF) superfamily, including APRIL, Blys/TALL-1, 4-1BBL, CD27L, CD30L, CD40L, FasL, GITRL, OX-40L, RANKL, TNF-α, or TRAIL/APO2L (*3*). Hypohidrotic (anhidrotic) ectodermal dysplasia (EDA) is a disorder characterized by the abnormal development of hair, teeth, and eccrine sweat glands (*4*). Mutations in the X-linked EDA gene, a distantly related member of the TNF-ligand superfamily, are responsible for most of the clinical cases studied to date (*5, 6*). A minority of patients with the EDA phenotype display an autosomal inheritance pattern that is due to mutations in a distinct gene, termed downless (dl) in mice and DL in humans (*7, 8*). The gene for EDA encodes various isoforms of a type II transmembrane protein, termed ectodysplasin. The longest form, EDA-A1, encodes a 391-residue protein with a domain similar to TNF at the COOH-terminus (*7–9*). Except for a two-residue deletion (Glu^{308} and Val^{309} in this domain), EDA-A2 is identical to EDA-A1. Genomic analysis of the EDA gene reveals that EDA-A2 is generated through the use of an alternative internal splice donor site (*10*). The Tabby (Ta) gene represents the ortholog of human EDA (*11, 12*). Virtually superimposable genomic organization and transcript profile have been described for Ta (*9*), implying evolutionary conservation.

To test whether EDA-A1 or EDA-A2 could be the ligand for XEDAR, we generated XEDAR-hFc, containing the extracellular domain of XEDAR fused to human immunoglobulin G1 Fc (hFc) (*13, 14*). Surprisingly, XEDAR-hFc bound cells that were transfected with full-length EDA-A2 but not cells transfected with EDA-A1, despite there only being a two–amino acid difference between these two molecules (Fig. 2A). The dl gene responsible for the autosomal form of EDA is predicted to encode a TNFR member, termed EDAR (*7, 8*). Genetic evidence suggests that EDAR is likely the receptor for EDA. We generated EDAR-hFc, consisting of the extracellular domain of EDAR fused to hFc (*13*). EDAR-hFc bound cells transfected with EDA-A1, the ligand possessing the extra two-residue insert (Glu^{308} and Val^{309}), but not cells transfected with EDA-A2 (Fig. 2A). This was the opposite of what was observed with XEDAR-hFc, which bound EDA-A2 but not EDA-A1. The reciprocal binding pattern was also demonstrable with soluble forms of ligands and cell surface–expressed receptors (Fig. 2B). Tagged soluble ligands were generated (*15, 16*) with human placental alkaline phosphatase (AP) or Flag-tag fused to the COOH-terminal regions of EDA-A1 and EDA-A2. AP-EDA-A1 and AP-EDA-A2 specifically stained cells transfected with EDAR or XEDAR, respectively (Fig. 2B). The binding of AP fusion proteins was specifically blocked by the corresponding Flag-tagged versions. Specific interactions of EDAR/EDA-A1 and XEDAR/EDA-A2 were confirmed by coimmunoprecipitation experiments (Fig. 2C). We also measured the binding of soluble ligand to immobilized receptor-Fc fusion protein (Fig. 2D). EDA-A2 exhibited an affinity for XEDAR similar to that of EDA-A1 for EDAR, both binding with an apparent dissociation constant of ~600 pM. Additionally, there was essentially no cross binding, even at high concentrations of ligand. Thus, the insertion of two amino acids in the ligand unequivocally dictated receptor binding specificity.

To better understand the nature of this molecular switch, we constructed models of EDA-A1 and EDA-A2 by sequence alignment and solved x-ray structures of family members, including lymphotoxin (*17*) and Apo2L/TRAIL (*18, 19*) as a template. The models (Fig. 2E) showed that the two-residue insert in EDA-A1 was predicted to be on the surface of the protein in an area expected to interact with the receptors (*3*). The extracellular region of XEDAR displays the highest sequence similarity to Troy (*20*), a recently identified orphan TNFR family member (Fig. 1A). Troy, however, did not bind either EDA-A1 or EDA-A2 (*3*).

Many TNFR family members activate the transcription factor nuclear factor κB (NF-κB). Upon transfection into 293 EBNA (293E) cells, XEDAR induced NF-κB activation (*3*). When the amount of input DNA was low, the small amounts of expressed XEDAR induced only minimal activation of NF-κB. However, NF-κB could be activated by exposure to the appropriate ligand (Fig. 3A). Even in the absence of XEDAR transfection, there was a weak activation of the NF-κB upon addition of purified Flag–EDA-A2 protein or transfection of EDA-A2, suggesting that 293E cells express low levels of endogenous receptor for EDA-A2 (Fig. 3, A and B). Treatment of untransfected 293E cells with purified Flag–EDA-A2 but not with Flag-EDA-A1 resulted in increased phosphorylation of inhibitor of nuclear factor κB–α (IκB-α), and this effect of Flag–EDA-A2 was specifically blocked by XEDAR-hFc but not by EDAR-hFc (Fig. 3C). Taqman analysis revealed a high level of XEDAR transcript in 293E cells. Additionally, a monoclonal antibody specific for XEDAR blocked EDA-A2–induced IκB-α phosphorylation (*3*). Thus, endogenous XEDAR is responsible for mediating NF-κB activation in 293E cells following exposure to EDA-A2.

Members of the TNF receptor–associated factor (TRAF) family mediate signaling by TNFRs. The cytoplasmic region of XEDAR bound TRAF1, TRAF3, and TRAF6 (*3*). The TRAF6 binding site was mapped to amino acids 252 to 260, and replacing Glu^{256} with Arg

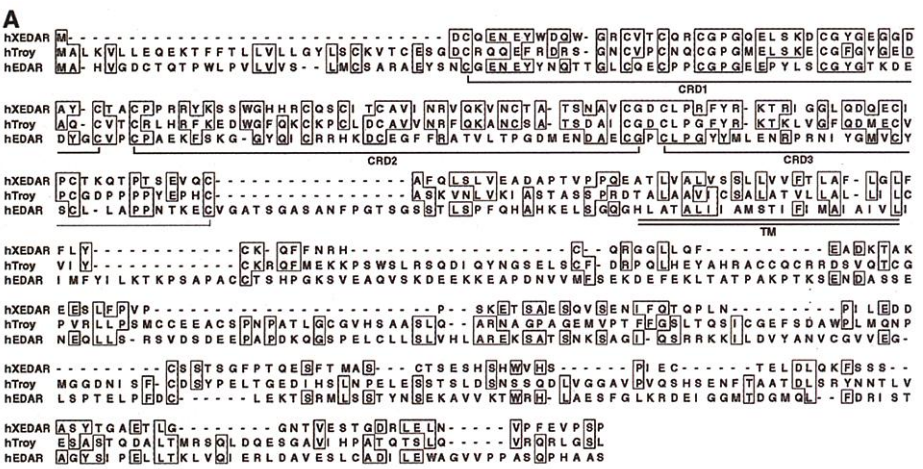

Fig. 1. XEDAR is a type III transmembrane protein of the TNFR superfamily. (**A**) Amino acid sequence of human XEDAR, Troy, and EDAR (*21*). The cysteine-rich repeat regions are underlined, and the predicted membrane-spanning region is doubly underlined. Conserved residues are boxed. (**B**) MCF-7 cells transiently transfected with XEDAR with either NH_2-terminal Flag tag (Flag-XEDAR) or COOH-terminal Flag tag (XEDAR-Flag) were immunostained with M2 antibody to Flag (Sigma), either with or without permeabilization with 0.5% Triton X-100.

abolished the binding of TRAF6 to XEDAR. Because the binding of TRAF6 (but not other TRAFs) to XEDAR correlated with activation of NF-κB (*3*), TRAF6 is likely a key adapter molecule in transducing XEDAR-mediated NF-κB signaling (Fig. 3D). In cells transfected with low amounts of TRAF6 and XEDAR, the interaction between the molecules was marginal. However, treatment with soluble Flag–EDA-A2 increased the recruitment of TRAF6 to XEDAR (Fig. 3E).

Transfection of EDAR into 293E cells also resulted in a dose-dependent activation of NF-κB (*3*). Unlike 293E cells, untransfected MCF7 cells do not respond to either EDA-A1 or EDA-A2 by activating the NF-κB pathway (Fig. 3F). In MCF7 cells, transfection of EDAR alone resulted in a dose-dependent activation of NF-κB. Synergistic activation of NF-κB was found upon cotransfection with EDA-A1. Furthermore, EDAR bearing the point mutation ($Arg^{420} \rightarrow Gln^{420}$) identified in a patient with an autosomal form of EDA (*8*) or the point mutation ($Glu^{379} \rightarrow Lys^{379}$) identified in dl mutant mice (*7*) was incapable of NF-κB activation (Fig. 3G), suggesting that engagement of the NF-κB pathway is critical for EDAR function. The cytoplasmic region of EDAR failed to bind any known TRAF molecules (*3*). Transient transfection of 293E cells with XEDAR, but not EDAR, activated the mitogen-activated protein kinase pathway as assessed by a luciferase-based Elk1 transcriptional assay (Fig. 3H).

We examined the expression of EDAR and XEDAR in developing mouse skin by in situ hybridization (Fig. 4A). At embryonic day 14 (E14), EDAR transcripts were clearly present in the basal cells of the developing epidermis, with elevated focal expression in placodes. XEDAR expression was barely discernable at this stage. However, by E16 and E17, both receptors were expressed in large amounts in the maturing follicles. By postnatal day 1 (P1), the pattern of expression was confined to the hair follicles.

We used the receptor Fc-fusion proteins to determine endogenous expression of EDA-A1 and EDA-A2 proteins in mouse skin. EDAR-hFc bound epidermis and hair follicles, but not dermal cells. Binding of XEDAR-hFc appeared later than that of EDAR-hFc and was mainly restricted to hair follicles (Fig. 4B). Detailed examination showed that EDA-A2 was more concentrated in the central core of the devel-

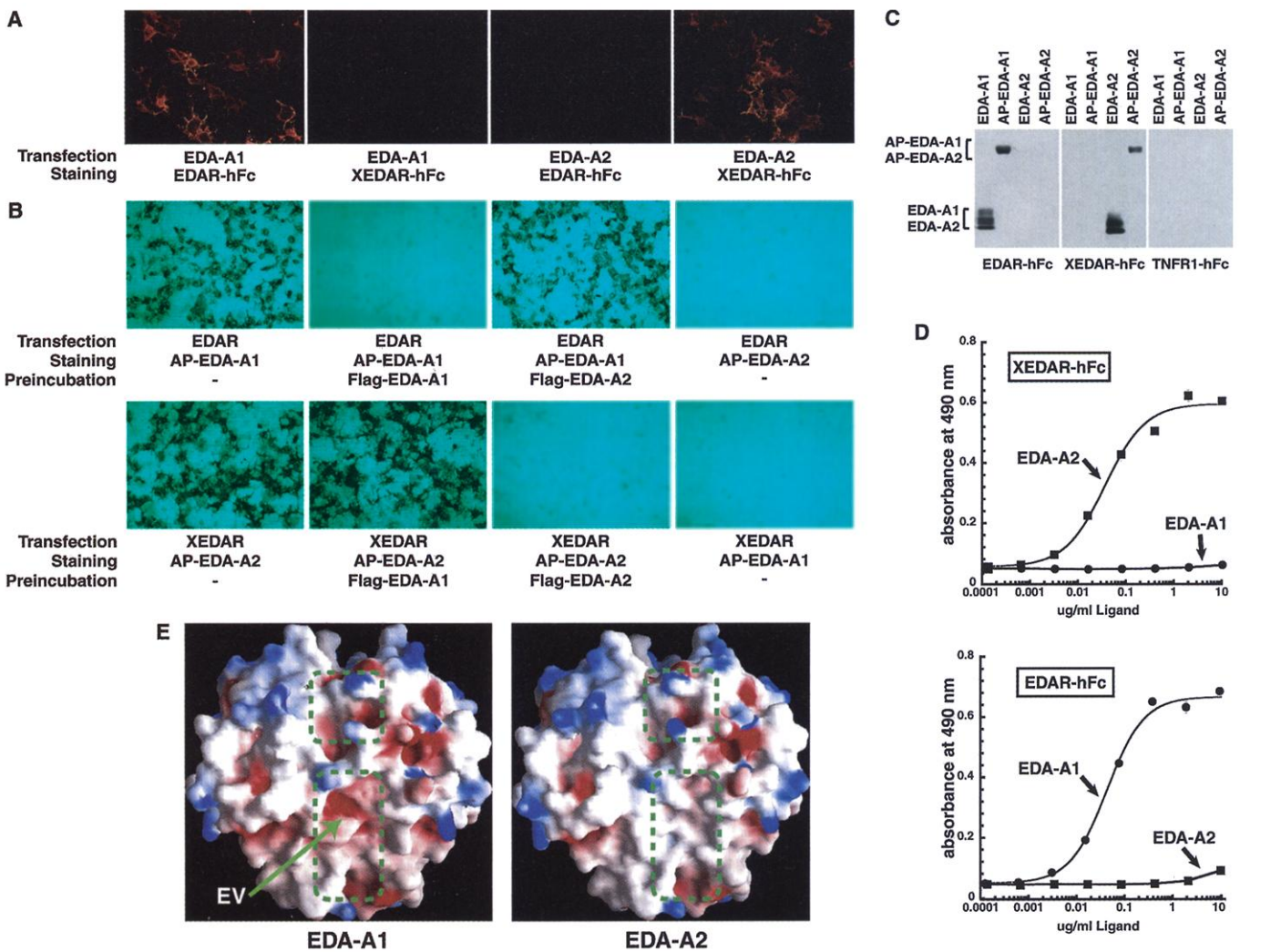

Fig. 2. Specific interactions of EDAR with EDA-A1 and XEDAR with EDA-A2. (**A**) COS-7 cells transfected with EDA-A1 or EDA-A2 were incubated with EDAR-hFc or XEDAR-hFc and stained with biotinylated goat antibody to human Fc and Cy3-streptavidin. (**B**) COS-7 cells transfected with either EDAR or XEDAR were stained with AP-EDA-A1 or AP-EDA-A2 (*16*). Where indicated, cells were preincubated with purified Flag-tagged ligand. (**C**) EDAR-hFc, XEDAR-hFc, or TNFR1-hFc was incubated with Flag-EDA-A1, Flag-EDA-A2, or conditioned medium containing Flag-AP-EDA-A1 or Flag-AP-EDA-A2. The immunoprecipitated receptor-Fc fusion proteins were subjected to anti-Flag Western blot. (**D**) Dosage-dependent binding of Flag-EDA-A1 and Flag-EDA-A2 to XEDAR-hFc (top) and EDAR-hFc (bottom) (*14*). (**E**) Molecular surfaces of models of EDA-A1 and EDA-A2 colored according to their calculated surface potential from −10 kT (red) to 0 kT (white) to 10 kT (blue). EV, Glu^{308} Val^{309}. The expected receptor contact regions are outlined in green. This figure was made with the program GRASP (*22*).

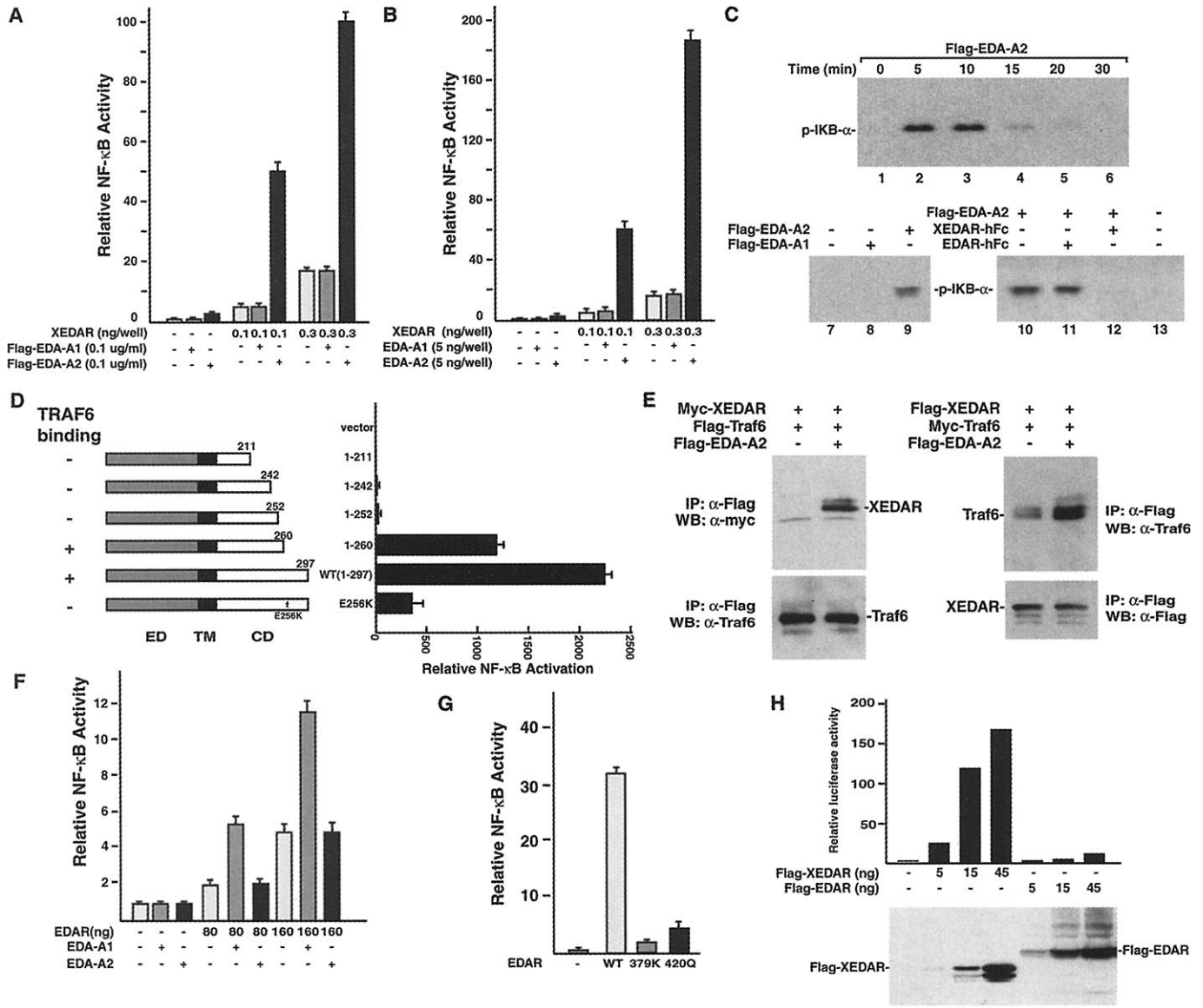

Fig. 3. Signal transduction mediated by EDAR and XEDAR. (**A** and **B**) Interaction of EDA-A2 with XEDAR results in activation of NF-κB. In (A), purified Flag-EDA-A1 or Flag-EDA-A2 was used; in (B), the cells were cotransfected with full-length EDA-A1 or EDA-A2. (**C**) Activation of NF-κB by treatment of EDA-A2 in untransfected 293E cells. Total cell lysates were subjected to Western blot using phosphospecific IκB-α antibody (New England BioLabs, Beverly, Massachusetts). (**D**) Analysis of XEDAR binding TRAF6 and activating NF-κB. XEDAR and its mutants were transiently transfected into 293E cells to measure their activities of NF-κB activation. Glutathione *S*-transferase fusion protein containing the cytoplasmic region of XEDAR or its variants was used to measure the interaction with Flag-TRAF6. E256K, $Glu^{256} \rightarrow Lys^{256}$; ED, extracellular domain; TM, transmembrane; CD, cytoplasmic domain; WT, wild type. (**E**) Ligand-dependent interaction between XEDAR and TRAF6. Low levels of differentially tagged XEDAR and TRAF6 were cotransfected into 293E cells. As indicated, cells were treated with purified Flag-EDA-A2 for 10 min before cells were lysed. IP, immunoprecipitation; WB, Western blotting. (**F**) Binding of EDA-A1 to EDAR results in activation of NF-κB in MCF7 cells. (**G**) Mutation in the cytoplasmic region of EDAR impairs EDAR-mediated NF-κB activation in 293E cells (*21*). (**H**) XEDAR but not EDAR mediates activation of Elk1 in 239E cells (PathDetect, Stratagene). Expression of receptor proteins was shown by anti-Flag Western blotting.

oping hair follicle, whereas EDA-A1 expression of EDA-A1 was circumferential (Fig. 4C). Regardless, the distinctive temporal and spatial expression of EDA-A1 and EDA-A2 suggest that they may have distinct roles in development of the hair follicle. In a skin organ culture system, both EDA-A1 and EDA-A2 increased the number of epidermal invaginations that are a precursor stage to mature hair follicles. EDA-A1 had a slightly higher activity than EDA-A2 (Fig. 4D).

Members of the TNFR family are important in immunity and inflammation. Our study indicates the involvement of this family in morphogenesis.

References and Notes

1. Human XEDAR was identified by searching a sequence database (Incyte Genomics, Lifeseq Gold; clone identification: INCY 5091511). Human XEDAR cDNA was cloned from a human fetal kidney library (GenBank accession number AF298812).
2. J. Wilson-Rawls, S. L. Deutscher, W. S. Wold, *Virology* **201**, 66 (1994).
3. M. Yan, V. Dixit, unpublished data.
4. N. Freire-Maia, M. Pinheiro, *Birth Defects Orig. Artic. Ser.* **24**, 3 (1988).
5. J. Kere *et al.*, *Nature Genet.* **13**, 409 (1996).
6. J. Zonana *et al.*, *Am. J. Hum. Genet.* **51**, 1036 (1992).
7. D. J. Headon, P. A. Overbeek, *Nature Genet.* **22**, 370 (1999).
8. A. W. Monreal *et al.*, *Nature Genet.* **22**, 366 (1999).
9. M. L. Mikkola *et al.*, *Mech. Dev.* **88**, 133 (1999).
10. M. Bayes *et al.*, *Hum. Mol. Genet.* **7**, 1661 (1998).
11. B. M. Ferguson *et al.*, *Hum. Mol. Genet.* **6**, 1589 (1997).
12. A. K. Srivastava *et al.*, *Proc. Natl. Acad. Sci. U.S.A.* **94**, 13069 (1997).
13. Human XEDAR (amino acids 2 to 154) was cloned into an expression vector engineered with an NH_2-terminal

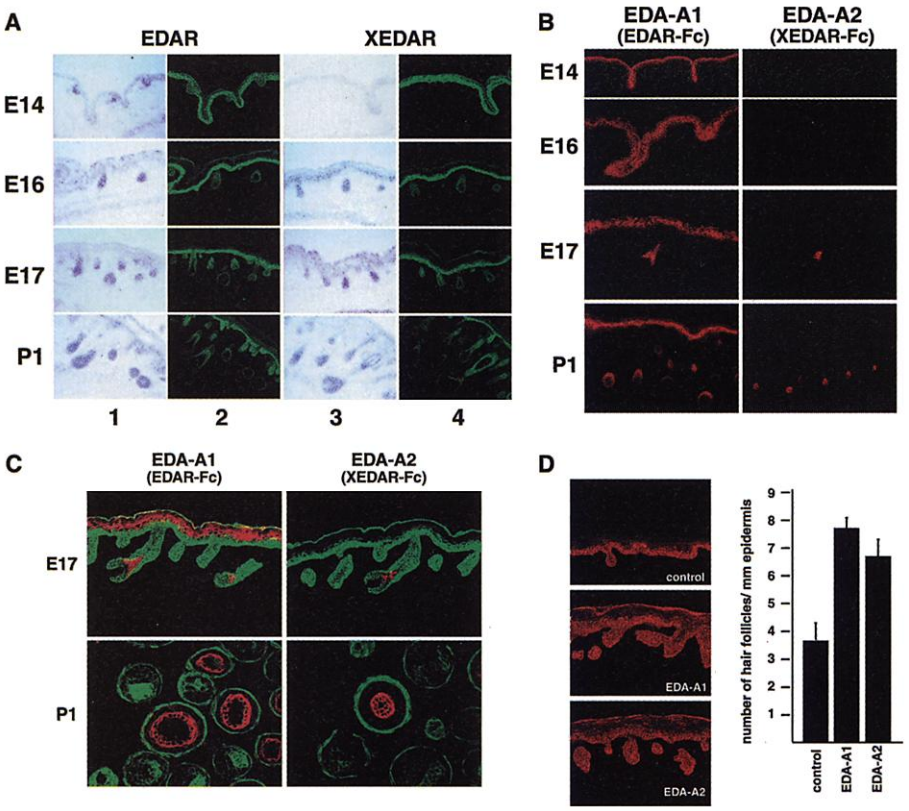

Fig. 4. Expression of EDAR, XEDAR, EDA-A1, and EDA-A2 in mouse skin. (**A**) Expressions of EDAR and XEDAR in mouse skin were examined by in situ hybridization (*23*). The digoxigenin-labeled riboprobes for mouse EDAR and XEDAR were synthesized corresponding to nucleotides 12 to 493 of the EDAR ORF and nucleotides 37 to 767 of the XEDAR ORF, respectively (1 and 3). The same sections were also immunostained with anti-keratin 5 (green) (2 and 4). (**B** and **C**) In situ staining of mouse skin with EDAR-hFc and XEDAR-hFc fusion proteins (red) (*24*). In (C), the mouse skin section was stained twice with anti-keratin 5 (green). A transverse view of P1 hair follicles shows that XEDAR-hFc and EDAR-hFc bind distinct regions. (**D**) Stimulation of epidermis downgrowths by EDA-A1 and EDA-A (*25*). Skin was dissected from CD-1 mouse embryos between E13.5 and E14.5 and cultured for 3 days in Dulbecco's modified Eagle's medium supplemented with 10% fetal bovine serum. Purified recombinant Flag-EDA-A1, Flag-EDA-A2, or Flag-Blys (control) was used at a final concentration of 0.2 μg/ml. Skin sections were then immunostained with anti-keratin 5 to assess the number of epidermal downgrowths. The average number of downgrowths per unit length of epidermis was calculated on the basis of a total of 18 organ cultures in three different experiments.

signal sequence derived from protrypsin and the hFc region downstream of the XEDAR sequence, resulting in XEDAR-hFc. EDAR-hFc was constructed by fusing the human EDAR (amino acids 1 to 189) to hFc.
14. S. A. Marsters *et al.*, *Curr. Biol.* **10**, 785 (2000).
15. Human EDA-A1 (amino acids 241 to 391) or EDA-A2 (amino acids 241 to 389) and human placental AP were amplified by polymerase chain reaction, fused, and cloned into the expression vector pFlag-CMV1 (Sigma) with AP at the NH_2-terminus of EDA-A1 or EDA-A2, respectively. Flag-EDA-A1 or Flag-EDA-A2 was constructed by cloning EDA-A1 (amino acids 179 to 391) or EDA-A2 (amino acids 179 to 389), respectively, into pFlag-CMV1.
16. J. G. Flanagan, P. Leder, *Cell* **63**, 185 (1990).
17. M. J. Eck, M. Ultsch, E. Rinderknecht, A. M. de Vos, S. R. Sprang, *J. Biol. Chem.* **267**, 2119 (1992).
18. S. G. Hymowitz *et al.*, *Biochemistry* **39**, 633 (2000).
19. S. S. Cha *et al.*, *Immunity* **11**, 253 (1999).
20. T. Kojima *et al.*, *J. Biol. Chem.* **275**, 20742 (2000).
21. Single-letter abbreviations for the amino acid residues are as follows: A, Ala; C, Cys; D, Asp; E, Glu; F, Phe; G, Gly; H, His; I, Ile; K, Lys; L, Leu; M, Met; N, Asn; P, Pro; Q, Gln; R, Arg; S, Ser; T, Thr; V, Val; W, Trp; and Y, Tyr.
22. A. Nicholls, K. A. Sharp, B. Honig, *Proteins* **11**, 281 (1991).
23. L. C. Wang, A. Shih, J. Hongo, B. Devaux, M. Hynes, *J. Neurosci. Res.* **61**, 1 (2000).
24. CD-1 mouse skin was freshly embedded in O.C.T. (optimal cutting temperature) compound, cryosectioned, and air-dried at room temperature for 5 min. The binding of receptor-hFc fusion proteins was visualized with Cy3-conjugated anti-human immunoglobulin G.
25. K. Foitzik, R. Paus, T. Doetschman, G. P. Dotto, *Dev. Biol.* **212**, 278 (1999).
26. We thank L. Closkey, P. Hass, and M. Nagel for help with recombinant protein expression and purification; R. Pitti for help with measuring the affinity of ligand-receptor interaction; K. O'Rourke for proofreading the manuscript; members in V.D.'s laboratory for discussions; and Genentech's antibody technology and DNA synthesis labs.

14 July 2000; accepted 12 September 2000

CD95/CD95 Ligand Interactions on Epithelial Cells in Host Defense to *Pseudomonas aeruginosa*

Heike Grassmé,[1] Susanne Kirschnek,[1] Joachim Riethmueller,[1] Andrea Riehle,[1] Gabriele von Kürthy,[2] Florian Lang,[1] Michael Weller,[2] Erich Gulbins[1]*†

Pseudomonas aeruginosa causes severe infections, particularly of the lung, that are life threatening. Here, we show that *P. aeruginosa* infection induces apoptosis of lung epithelial cells by activation of the endogenous CD95/CD95 ligand system. Deficiency of CD95 or CD95 ligand on epithelial cells prevented apoptosis of lung epithelial cells in vivo as well as in vitro. The importance of CD95/CD95 ligand–mediated lung epithelial cell apoptosis was demonstrated by the rapid development of sepsis in CD95- or CD95 ligand–deficient mice, but not in normal mice, after *P. aeruginosa* infection.

Several pathogens, including some bacteria, viruses, and parasites, are able to trigger apoptosis of mammalian host cells (*1*, *2*). A paradigm for bacteria-induced apoptosis is *Shigella flexneri*, which, upon invasion, induces apoptosis by the activation of caspases (in particular, caspase 1) (*3*). Some other bacteria also induce apoptosis, including *Salmonella typhimurium*, some enteropathogenic *Escherichia coli*, *Listeria monocytogenes*, and *Staphylococcus aureus* (*4*–*7*). However, the molecular mechanisms involved and their relevance to host pathogen interactions are still largely unknown.

P. aeruginosa is clinically one of the most important classes of bacteria, because it induces pneumonia and sepsis in cystic fibrosis or immunocompromised patients. To gain insight into the molecular mecha-

[1]Department of Physiology, University of Tuebingen, Gmelinstrasse 5, 72076 Tuebingen, Germany. [2]Department of Neurology, University of Tuebingen, Hoppe-Seyler Strasse 3, 72076 Tuebingen, Germany.

*Present address: Department of Immunology, St. Jude Children's Research Hospital, 332 North Lauderdale Street, Memphis, TN 38105, USA.

†To whom correspondence should be addressed. E-mail: erich.gulbins@stjude.org